THE ASTROPHYSICAL JOURNAL, 470:378–393, 1996 October 10

THE DISAPPEARING BROAD ABSORPTION LINES AND VARIABLE EMISSION LINES IN NGC 3516

ANURADHA KORATKAR,[1] MICHAEL R. GOAD,[1,2,3] PAUL T. O'BRIEN,[4,5] ISABEL SALAMANCA,[3,6]
IGNAZ WANDERS,[7,8] DAVID AXON,[9,10] D. MICHAEL CRENSHAW,[11] ANDREW ROBINSON,[12,13]
KIRK KORISTA,[14] PEDRO RODRÍGUEZ-PASCUAL,[15] KEITH HORNE,[1,16] JIM BLACKWELL,[11]
MICHAEL CARINI,[17] MARTIN ENGLAND,[17] MARIO PEREZ,[17]
RONALD PITTS,[17] LLOYD RAWLEY,[17] GAIL REICHERT,[18]
CHRIS SHRADER,[19] AND WILLEM WAMSTEKER[15]

Received 1995 November 17; accepted 1996 April 25

ABSTRACT

The Seyfert 1 galaxy NGC 3516 was monitored during 1993 February 16–May 13 by *IUE* every 4 days for the first month, and then every 2 days for 2 months giving a total of 40 observations. This paper gives the initial results from this campaign. (1) The broad C IV λ1549 emission line variations are delayed relative to those of the ionizing continuum by ~4.5 days, consistent with that of other similar luminosity active galactic nuclei. (2) The mean 1993 UV continuum level was about a factor of 3 higher than the mean archive spectrum and was at a record level throughout the campaign. (3) There was dramatic variability in the C IV λ1549 line profile when compared to the *IUE* archival data. A narrow absorption line is present in all of the 1993 spectra. In contrast, the broad variable trough was undetectable, whereas it is a very strong feature in all of the *IUE* archival spectra. The N V λ1240 and Si IV λ1400 lines showed a similar behavior.

A variable broad absorption line (VAL) model is required to explain the archival data, but it is unclear if a VAL model alone can explain the 1993 *IUE* data. Photoionization models suggest that the lack of line troughs in 1993 cannot be caused simply by increased ionization of the VAL gas. We propose two distinct models to explain the 1993 spectra: either the VAL gas has been dissipated, leaving a narrow absorption line presumably due to a more distant absorber, or an emission component, possibly a bicone, has greatly increased its contribution to the blue wing. Dissipation of the VAL gas implies a dynamic absorber, possibly the ionized surface layer of a molecular torus. An extra emission component implies that the broad line region properties in NGC 3516 may be radically different than has hitherto been proposed.

Subject headings: galaxies: active — galaxies: individual (NGC 3516) — galaxies: Seyfert — ultraviolet: galaxies

1. INTRODUCTION

One of the central problems in the field of active galactic nuclei (AGNs) research is to understand the nature of the broad line region (BLR). Over the past decade it has become clear that monitoring the response of the emission line gas to ionizing continuum variations is a very powerful method for determining the size, structure, and kinematics of the BLR (see Peterson 1993 for a review). Broad emission line variability occurs in AGNs covering a wide range in luminosity. The emission line variations are delayed relative to those of the continuum by characteristic timescales which range from a few months in high-luminosity quasars (O'Brien & Harries 1991) down to a few days in low-luminosity Seyfert 1 galaxies (Clavel et al. 1990, 1991; Koratkar & Gaskell 1991a, 1991b; Korista et al. 1995). These time delays, or lags, are usually interpreted in terms of the time-delayed response of the spatially extended BLR to the ionizing continuum source (Peterson 1993).

About 10% of all QSOs are broad absorption line (BAL) QSOs, in that in addition to broad emission lines, they have broad absorption lines blueward of line center (extending to -10^4 km s^{-1}) with large equivalent widths (typically 40 Å for C IV) that appear to be intrinsic to the nucleus. In most other respects the BAL QSOs appear to be normal (see Weymann et al. 1991). The precise relationship between the

[1] STScI, 3700 San Martin Drive, Baltimore, MD 21218.
[2] Rutherford Appleton Laboratory, Didcot, Oxon, OX11 0QX, UK.
[3] Department of Physics and Astronomy, University College London, Gower Street, London, WC1E 6BT, UK.
[4] Astrophysics, Department of Physics, University of Oxford, Keble Road, Oxford, OX1 3RH, UK.
[5] Department of Physics and Astronomy, University of Leicester, University Road, Leicester, LE1 7RH, UK.
[6] Observatoire de Paris-Meudon, URA 173, 92195 Meudon Cedex, France.
[7] Uppsala Astronomical Observatory, Box 515, S-75120, Uppsala, Sweden.
[8] Department of Astronomy, Ohio State University, 174 West 18th Avenue, Columbus, Ohio, OH 43210.
[9] Affiliated to the Space Science Division of ESA, STScI, 3700 San Martin Drive, Baltimore, MD 21218.
[10] Nuffield Radio Astronomy Laboratory, University of Manchester, Jodrell Bank, Macclesfield, Cheshire, SK11 9DL, UK.
[11] Computer Sciences Corporation, Laboratory for Astronomy and Solar Physics, NASA/GSFC, Code 681, Greenbelt, MD 20771.
[12] Department of Physical Sciences, University of Hertfordshire, College Lane, Hatfield, Hertfordshire, AL10 9AB, UK.
[13] Institute of Astronomy, Madingley Road, Cambridge, CB3 0HA, UK.
[14] Department of Physics and Astronomy, University of Kentucky, Lexington, KY 40506.
[15] ESA *IUE* Observatory, P.O. Box 50727, 28080 Madrid, Spain.
[16] Physics and Astronomy, University of St. Andrews, North Haugh, St. Andrews, KY16 922, UK.
[17] Computer Sciences Corporation, *IUE* Observatory, NASA/GSFC, Code 684.9, Greenbelt, MD 20771.
[18] Universities Space Research Association, NASA/GSFC, Code 668, Greenbelt, MD 20771.
[19] Computer Sciences Corporation, *GRO* Science Support Center, NASA/GSFC, Code 668.1, Greenbelt, MD 20771.

emission and absorption line gas is unclear. However, there is mounting evidence that most, and possibly all, radio-quiet QSOs have BAL gas with a small covering factor (Weymann et al. 1991; Stocke et al. 1992; Hamann et al. 1993). About 3% of Seyfert 1 galaxies observed with *IUE* show similar line profiles, suggesting the existence of similar, although somewhat narrower, broad absorption troughs. These features are also blueshifted (extending to ~ -3000 km s^{-1}) and have equivalent widths in the range 4–10 Å (Ulrich 1988). The relationship between these two types of AGN and between the emission and absorption line regions in general is unclear, but the Seyfert galaxies with absorption features may be a low-luminosity manifestation of the BAL QSO phenomenon (Shull & Sachs 1993). Since Seyfert 1 galaxies are believed to be the low-luminosity analogs of QSOs, the study of these objects should provide information on the physical properties of the emission and absorption line regions in AGN.

Only three Seyfert 1 galaxies believed to exhibit variable absorption features have been studied in any detail in the UV, and the true nature of the absorbing gas remains elusive. For NGC 4151 the absorbing gas seems to consist of a large number of high-density ($>10^9$ cm^{-3}) optically thin clouds, lying just outside the BLR (Bromage et al. 1985; Kriss et al. 1992)—properties similar to those derived for BAL QSOs (Korista et al. 1992).

For NGC 5548, Shull & Sachs (1993) assuming that C IV was the dominant stage of ionization, used UV observations to deduce that the absorption was produced by optically thin, weakly ionized ($U \sim 10^{-3}$), low-density ($n_e \geq 5 \times 10^5$ cm^{-3}) clouds, located outside ($r \sim 14$ pc) and partially obscuring the BLR. Combined with the lack of Mg II and Lyα absorption they placed an upper limit on the column density of $N_{\rm H} < 10^{20.5}$ cm^{-2}. Mathur et al. (1995) in an attempt at linking the X-ray and UV absorbers into a single coherent model, combined X-ray observations of O VII and O VIII absorption edges (Fabian et al. 1994) with the UV observations to deduce that the absorption arises in highly ionized ($2.2 < U < 2.8$), high column density $n_{\rm H} = 3.8 \times 10^{21}$ cm^{-2} clouds located at a distance of between 8 light-days and one light-year from the ionizing continuum source. The detection of Lyα absorption in the 1993 *HST* spectra of NGC 5548, and in a reanalysis of the archival *IUE* data allowed them to place limits on the H I column of 10^{13} cm$^{-2} < N_{\rm H\,I} < 10^{18}$ cm^{-2}. Although their results are consistent with the observed anticorrelation in the EW (C IV) with the continuum at λ1750 Å, their "single-cloud" model underestimates the observed Fe K emission by a factor of 25. This suggests that either the link between the UV and X-ray absorbers is rather tenuous or that a "single-cloud" model for the absorbing gas is inappropriate.

For NGC 3516 the situation, as summarized below, is far less clear (Voit, Shull, & Begelman 1987; Walter et al. 1990; Kolman et al. 1993). Ulrich (1988) noted that NGC 3516 has the strongest (largest equivalent-width) and most variable ultraviolet absorption line spectrum of the Seyfert 1 galaxies observed by *IUE*, making it a key test-case for AGN models.

The variability of NGC 3516 in the optical, UV and X-rays has been previously reported by Ulrich & Boisson (1983); Voit et al. (1987); Walter et al. (1990); Bochkarev, Shapovalova, & Zherov (1990); Krupper, Urry, & Canizares (1990); and Kolman et al. (1993). The UV continuum in NGC 3516 has varied by a factor of 4 in the *IUE* archival data. Both the broad emission and absorption lines vary on timescales of a few days to weeks, with significant variations seen on 2 consecutive days of observations. Walter et al. find that the intensity of the broad base of the C IV emission line correlates very well with the UV continuum, whereas the narrow emission core varies little if any. They also find that the C IV absorption line can be represented by a narrow stable component and a variable broad absorption line (VAL).

As part of its AGN BLR monitoring campaign, the European "LAG" collaboration observed NGC 3516 at 22 epochs between 1990 January and June using the 2.5 m Isaac Newton and the 4.2 m William Herschell telescopes on La Palma (Wanders et al. 1993). Significant optical continuum and Balmer line variability occurred on timescales as short as the minimum sampling interval of 2–3 days. The cross-correlation functions indicate a small BLR size of about 14 and 11 light-days for Hα and Hβ, respectively, which is somewhat smaller than the 25 light-days derived by Cherepashchuck & Lyutyi (1973). The quality of the LAG dataset is good enough to detect fairly small line profile variations. On the shortest observed timescales, symmetric variations occurred across the entire line profile. However, on timescales of a few weeks, asymmetric profile changes occurred, with significantly more variability in the blue compared to the red wing (Wanders et al. 1993; Wanders & Horne 1994). Although, Hα and Hβ appear to vary in a similar fashion overall, there were some detailed differences. In particular, a dip in the Hβ profile which formed during the LAG campaign was not seen in Hα, even after allowing for contamination by narrow [N II] λ6548 (Wanders et al. 1993). The Hβ dip coincides in velocity (-1300 km s^{-1}) with that of the UV absorption lines seen in the archival *IUE* data. Unfortunately there were no UV spectra of NGC 3516 taken during the LAG campaign for comparison.

A response function analysis of the LAG campaign Hα data (Wanders & Horne 1994) suggests that either the Balmer line emitting BLR geometry of this object is nonspherical or that the continuum and/or line emission is highly anisotropic. Wanders & Horne (1994) also find that the Hα response function is nonstationary, most likely due to variations in the spectral energy distribution, nonlinear line response, cloud destruction/formation or time-dependent variations in the source anisotropy. The velocity resolved Hα response function shows a similar structure across a broad range in velocity space, ruling out radial motion as dominating the Balmer line emitting gas kinematics in NGC 3516.

Although the archival *IUE* data and the optical data showed that variability occurs in NGC 3516 on timescales of less than a few weeks, we were severely hampered in our understanding of the emission and absorption line regions in this AGN due to the lack of a well sampled UV data set. To better constrain the emission line properties (e.g., the size of the BLR and the gas kinematics), and the properties of the absorption line region (e.g., cloud density and size, viability of the Walter et al. [1990] absorbing cloud model), we organized an intensive *IUE* monitoring campaign during 1993. The principal objectives of the campaign were as follows: (1) determine the structure of the broad emission line region, and compare it to other AGNs; (2) determine the origin of the broad trough in the C IV line (i.e., is it due to absorption or just a lack of emission); and (3) determine

the continuum variability characteristics. In this paper we present the 1993 *IUE* data and the first results deduced from the observed UV emission and absorption line variability.

2. OBSERVATIONS AND DATA REDUCTION

2.1. *Observing Strategy*

The *IUE* archival data of NGC 3516 showed that the UV continuum and high ionization lines are variable on timescales of a few days. However, the optical data showed that low ionization line variability occurs on timescales of a week. Because of this dichotomy in response times for the low- and high-ionization lines, we monitored NGC 3516 with *IUE* during 1993 February–May every 4 days for the first month and then every 2 days for 2 months. For most of the observations, we obtained an SWP exposure during a single half-shift, due to our interest in the rich C IV emission and absorption line spectrum. LWP exposures were also obtained at two epochs. All the observations were obtained through the large apertures (10″ × 20″) in low-dispersion mode.

The *IUE* observations were greatly complicated by the presence of scattered solar light in the telescope tube (Carini & Weinstein 1992), which has been present since 1991 and is particularly intense at high β's, where β is the angle between the telescope axis and the antisolar direction. Since NGC 3516 is always at $\beta > 60°$, there is no way to avoid this problem. However, the scattered light spectrum is such that although it can contaminate the long-wavelength region of the LWR/P cameras, there is a negligible contribution in the SWP.

The most important effect of the scattered light for this study was in greatly increasing the background level in the optical target acquisition detector, the FES. This had two consequences: first, the nucleus of NGC 3516 could not be detected directly (hence no optical light curve was obtained), but rather had to be acquired by blind offset from a nearby SAO star. The expected positioning error for this procedure is less than 1″. Second, and more importantly, the lack of bright guide stars in the relatively small portion of the FES field of view that was not severely affected by the scattered light make it impossible to guide during exposures. Thus, each exposure was accumulated in segments of duration 10 to 40 minutes under gyro control. Between each segment, the telescope was slewed to bring a nearby star to the position in the FES field least affected by scattered light in order to update the telescope pointing and the gyro rates. The "drift error," or difference in expected and found positions of the star after each segment, was determined in both the FES X and Y directions and represents the maximum drift of the target in the aperture during that segment. In fact, it is most likely an overestimate given the two slews to and from the guide star each time. Most of the drift errors were less than 3″ in the X direction (nearly perpendicular to the dispersion) and 1.″5 in the Y direction (nearly parallel to the dispersion). These drift errors potentially adversely affect both the photometric and wavelength accuracy of the data. However, using the optimal extraction techniques described in § 2.3, the impact on the photometric accuracy is only important if a large portion of the point-spread function (PSF) drifts outside of the aperture. The dimensions of the large apertures are 20″ in the X direction and 10″ in the Y direction, whereas the FWHM of the PSF is about 3″ (Cassatella, Barbero, & Benvenuti 1985). Thus, the photometric accuracy is only significantly affected if the target drifts more than about 8″ in the X direction and 3″ in the Y direction. The drift errors were very rarely larger than these values (§ 2.2), so the photometric integrity of the data was well maintained. The wavelength scale is affected mainly by drifts in the Y direction. The zero point of the dispersion relation can be corrected by aligning the spectra, but Y drift errors can also smear out spectral lines. Fortunately, this effect is relatively minor in our data, since a typical drift of 1.″5 translates to a wavelength shift of only 1.65 Å in an SWP spectrum (Bohlin et al. 1980), whereas the width of the SWP PSF is 5–7 Å (Cassatella et al. 1985). No significant differences in the width of the narrow C IV λ1549 absorption line were detected amongst any of the 1993 spectra.

2.2. *Log of Observations*

The 38 SWP and 2 LWP spectra obtained for this program are described in Table 1. The date, time, and Julian Date all refer to the beginning of the first segment. The duration refers to the sum of exposure times for all of the segments, although the total elapsed time for the observations was as much as a factor of 2 longer due to the target acquisition and guiding procedure described in § 2.1. The notes for Table 1 indicate problems with individual observations. Images SWP 47350, SWP 47596, and SWP 47607 are not used in this study since the exposures were blank, very weak, or contaminated by a guide star. Only SWP 47642 and LWP 25251 had significant drift errors for a large fraction of the exposure time. However, the flux for the SWP spectrum is consistent with that measured at the adjacent epochs, and it was therefore included in this study. LWP 25251 is badly contaminated by scattered light at long wavelengths (>3000 Å), but is totally consistent with LWP 24932 at shorter wavelengths.

2.3. *Ultraviolet Spectral Extraction*

Spectra were extracted from each of the 40 IUESIPS[20] line-by-line files using the optimal extraction technique of Kinney, Bohlin, & Neill (1991), which has been incorporated into the *IUE* Final Archive processing system, NEWSIPS, developed by NASA/ESA/SERC (Nichols-Bohlin 1993). Details of the optimal extraction procedure can be found in Kinney et al. (1991), and here we merely summarize the major points. Empirical spline fits are made to the cross-dispersion point spread function (PSF) along the spectrum, which constrains the PSF to vary smoothly in the dispersion direction. This constraint improves the signal-to-noise of the extracted spectrum relative to the standard IUESIPS, whilst still conserving flux. The flux at each wavelength is then determined by fitting the empirically determined profile, sample by sample, weighted according to a noise model determined from studies of hundreds of *IUE* images. Discrepant points are removed by clipping at $\pm 3\ \sigma$, which automatically removes most of the cosmic rays unless they happen to fall at the center of the cross-dispersion profile. A net flux uncertainty is associated with each flux value based on the noise model. Extensive comparisons of the optimal extraction and IUESIPS, show

[20] A detailed description of IUESIPS, the "*International Ultraviolet Explorer* Spectral Image Processing System" can be found in Clavel et al. (1991).

TABLE 1

NEW *IUE* OBSERVATIONS OF NGC 3516

Image Number	UT Date (month/day/year)	UT Start (hour:minute:second)	Julian Date (2440000+)	Duration (minutes)	Notes
SWP 46972.....	02/16/93	14:21:11	9035.098	210	
LWP 24932.....	02/16/93	19:16:54	9035.304	70	a
SWP 47009.....	02/20/93	13:59:36	9039.083	145	
SWP 47043.....	02/24/93	14:22:07	9043.099	107	
SWP 47072.....	02/28/93	06:26:14	9046.768	240	
SWP 47092.....	03/04/93	04:09:57	9050.674	125	
SWP 47127.....	03/06/93	09:11:69	9052.884	69	
SWP 47241.....	03/10/93	08:58:42	9056.873	85	
SWP 47266.....	03/12/93	07:49:46	9058.827	120	
SWP 47275.....	03/14/93	07:56:52	9060.832	115	
SWP 47325.....	03/20/93	15:47:56	9067.158	90	
SWP 47334.....	03/22/93	15:36:49	9069.151	80	
SWP 47350.....	03/24/93	16:07:02	9071.172	98	b
SWP 47365.....	03/26/93	15:29:13	9073.146	110	
SWP 47381.....	03/28/93	15:04:25	9075.128	175	
SWP 47392.....	03/30/93	22:41:13	9077.445	195	
SWP 47401.....	04/01/93	13:56:03	9079.081	180	
LWP 25251.....	04/01/93	17:43:54	9079.239	60	c
SWP 47413.....	04/03/93	17:36:03	9081.233	120	
SWP 47433.....	04/07/93	02:01:14	9084.584	160	
SWP 47449.....	04/09/93	06:02:25	9086.751	135	
SWP 47460.....	04/11/93	07:14:13	9088.802	65	
SWP 47475.....	04/13/93	06:00:00	9090.750	130	
SWP 47489.....	04/15/93	13:44:48	9093.073	130	
SWP 47497.....	04/17/93	14:18:52	9095.097	100	
SWP 47506.....	04/19/93	13:35:48	9097.067	140	
SWP 47518.....	04/21/93	13:51:51	9099.078	155	
SWP 47533.....	04/23/93	13:36:09	9101.067	160	
SWP 47545.....	04/25/93	13:42:14	9103.071	160	
SWP 47558.....	04/27/93	13:14:38	9105.052	180	
SWP 47569.....	04/29/93	13:11:32	9107.050	175	
SWP 47578.....	05/01/93	12:17:50	9109.013	105	
SWP 47596.....	05/03/93	13:49:34	9111.076	4	d
SWP 47605.....	05/04/93	20:14:52	9112.344	105	
SWP 47607.....	05/05/93	05:30:48	9112.729	20	e
SWP 47617.....	05/06/93	23:55:02	9114.496	165	
SWP 47628.....	05/09/93	00:11:32	9116.508	145	
SWP 47642.....	05/11/93	03:59:56	9118.667	140	c
SWP 47656.....	05/12/93	04:04:32	9119.670	140	
SWP 47661.....	05/13/93	04:39:15	9120.694	95	

[a] Mg II overexposed.
[b] Blank exposure. Target not in aperture due to anomaly.
[c] Error = 9".5 in X direction for one 40 minute segment.
[d] Very weak exposure. Cosmic-ray hit at C III].
[e] Very weak exposure. Contaminated by guide star.

no systematic disagreement in extracted net fluxes between the two techniques (Kinney et al. 1991).

To allow for drifts in the spatial direction due to the gyro guiding, and hence maintain photometric accuracy, the spectra were extracted using the 15 line optimal extraction routine rather than the standard 9 line extraction. The extracted net fluxes were converted to absolute fluxes using the *IUE* calibration of Bohlin et al. (1990). A correction was made for the SWP sensitivity degradation (Bohlin & Grillmair 1988), as updated through 1992.5 by R. C. Bohlin (1995, private communication). The linear extrapolation to 1993 epochs should not cause absolute flux errors of more than 1%. The LWP sensitivity degradation was similarly corrected for using data extrapolated from Teays & Garhart (1990). The use of segmented exposures did result in less on-target exposure time, and hence a lower exposure level than originally desired, although this was partly compensated for by the optimal extraction procedure. The broader spatial PSF potentially introduces more fixed-pattern noise, which is hard to estimate.

2.4. *Flux Measurements and Spectral Fitting*

As it is difficult to isolate the C IV emission line component in NGC 3516 due to the presence of the absorption line, the C IV flux during the campaign was simply measured by integrating above an eye estimated straight line fit to continuum windows located either side of the line.

The observed line fluxes at each epoch are given in Table 2, and refer to a rest-frame wavelength interval of 1500–1600 Å. The observed continuum fluxes at 1450 Å (rest-frame) are also given in Table 2, and both are plotted on a relative flux scale in Figure 1. This technique clearly measures only the change in the total C IV flux, and does not indicate any relative change between the absorption and emission line components.

To investigate the long term nuclear variability of NGC 3516, we have also included the archival *IUE* spectra in our analysis. A few archival spectra were unavailable for reextraction, but their omission does not affect our conclusions. The archival spectra were extracted and flux calibrated as

TABLE 2

FLUX MEASUREMENTS

Julian Date (2440000+)	Flux at 1450 (10^{-16} ergs s^{-1} cm^{-2} Å^{-1})	Flux in C IV (10^{-14} erg cm^{-2} s^{-1})	Notes
9035.098	490.6 ± 7.7	370.7 ± 4.5	
9039.083	481.9 ± 7.7	422.8 ± 5.0	
9043.099	526.1 ± 10.8	286.6 ± 6.1	a
9046.768	495.1 ± 6.7	378.9 ± 4.3	
9050.674	534.5 ± 7.8	344.8 ± 4.8	
9052.884	560.5 ± 12.0	367.7 ± 6.8	
9056.873	518.1 ± 10.5	402.3 ± 6.4	
9058.827	487.3 ± 8.4	420.9 ± 5.3	
9060.832	413.3 ± 7.9	337.6 ± 4.9	
9067.158	383.9 ± 9.1	369.6 ± 5.6	
9069.151	409.7 ± 9.6	304.4 ± 6.0	
9073.146	468.6 ± 9.1	333.5 ± 5.2	
9075.128	478.7 ± 7.3	333.5 ± 4.4	
9077.445	524.4 ± 7.2	335.3 ± 4.3	
9079.081	468.0 ± 6.9	391.7 ± 4.4	
9081.233	480.5 ± 12.2	386.3 ± 7.1	
9084.584	507.7 ± 7.6	408.2 ± 4.7	
9086.751	542.0 ± 8.2	406.1 ± 5.3	
9088.802	507.3 ± 11.4	386.4 ± 6.9	
9090.750	605.0 ± 8.6	395.8 ± 5.3	
9093.073	706.5 ± 9.5	410.0 ± 5.6	
9095.097	556.3 ± 12.5	301.8 ± 6.8	a
9097.067	543.7 ± 8.7	438.1 ± 5.6	
9099.078	503.0 ± 8.5	406.4 ± 5.3	
9101.067	547.8 ± 8.3	390.2 ± 5.0	
9103.071	638.1 ± 11.5	317.4 ± 5.5	a
9105.052	554.9 ± 8.0	396.5 ± 5.1	
9107.050	461.2 ± 7.7	375.3 ± 4.7	
9109.013	507.2 ± 8.8	385.4 ± 5.4	
9111.076	464.3 ± 15.1	363.5 ± 8.2	b
9112.344	493.3 ± 8.5	362.6 ± 5.3	
9112.729	509.2 ± 31.3	310.2 ± 15.8	b
9114.496	470.9 ± 7.1	359.5 ± 4.5	
9116.508	527.1 ± 7.9	323.7 ± 4.9	
9118.667	515.2 ± 8.5	373.3 ± 5.1	
9119.670	532.8 ± 8.7	270.2 ± 5.0	
92120.694.....	541.6 ± 9.8	375.9 ± 5.9	

[a] Low continuum and high radiation background spectra.
[b] Very weak exposure.

described in § 2.3. The line profiles appear to be correlated with the continuum flux in the archival spectra. This implies that we can form average archival SWP and LWP spectra which provide snapshots of the "steady state" BLR emission as a function of continuum level (see below). Similarly, given the stability of the C IV profile and the relatively small continuum flux range during the 1993 campaign, we formed an average spectrum (titled *campaign*, see Fig. 2*a*) to provide a snapshot of the BLR emission corresponding to a very-high continuum state. Due to the scattered light in LWP 25251, the average campaign LWP spectrum is actually only LWP 24932 (see Fig. 3*a*). It should be noted that, as the continuum level is not a monotonic function of time, the average spectra do not represent a chronological sequence. Apart from a few spectra with small global wavelength shifts due to errors in the target acquisition procedure, there were no significant shifts in the position of the red peak of the C IV line within the instrumental resolution. Therefore, the individual SWP spectra were all aligned relative to the C IV red peak before forming the average spectra. This procedure also brought the He II and C III] peaks into very good agreement between the average spectra. The LWP spectra were not aligned.

The SWP and LWP archival spectra were averaged into three groups, depending on the 1450 Å continuum flux at each epoch. The spectra used are given in Tables 3 and 4, and shown in Figures 2*b* and 3*b*. The first average achival spectrum (titled *archival-low*) was generated from 8 SWP spectra and 2 LWP spectra with continuum fluxes $f_\lambda < 1 \times 10^{-14}$ erg s^{-1} cm^{-2} Å^{-1}. The second average archival spectrum (titled *archival-mid*) had 19 SWP and 6 LWP spectra with continuum fluxes in the range 1–2 $\times$ 10^{-14} erg s^{-1} cm^{-2} Å^{-1}. The third average archival spectrum (titled *archival-high*) had 8 SWP and 5 LWP spectra with continuum fluxes in the range 2–3 $\times$ 10^{-14} erg s^{-1} cm^{-2} Å^{-1}. An average of all the archival spectra was also formed (titled *mean archival*, see Figs. 2*a* and 3*a*).

Although the archival LWR spectra were extracted, they are not included in our analysis as they have systematically lower signal-to-noise ratio than the LWP spectra in the region of the Mg II λ2798 line. Including the LWR spectra would not significantly affect the archival-low or archival-high spectra, and would increase the archival-mid continuum by only 20%.

The fluxes and equivalent widths of the major emission lines in the average spectra are given in Table 5. The flux measurements are all relative to a locally defined continuum. The C IV λ1549, He II λ1640, and C III] λ1909 line fluxes were measured between wavelength intervals of 1515–1610 Å, 1610–1700 Å and 1870–1950 Å observed

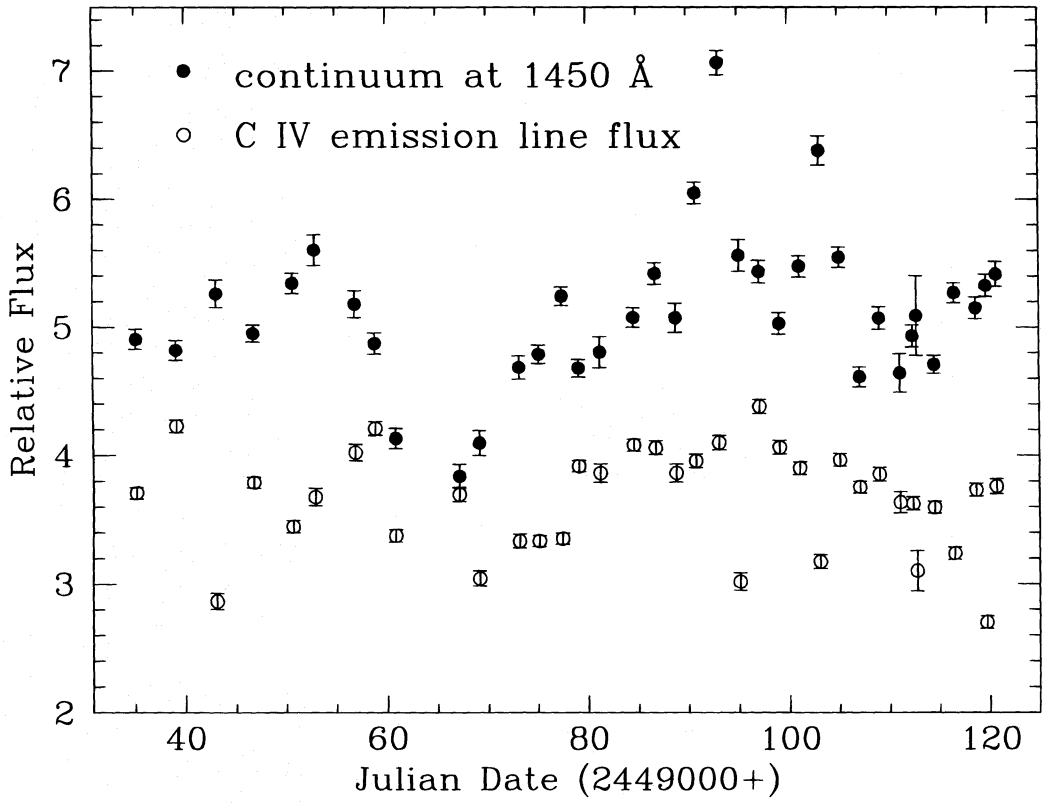

FIG. 1.—Time series for the continuum (*filled circles*) and the C IV line flux data (*open circles*) for the 1993 monitoring data. The continuum flux is in units of 10^{-14} erg cm^{-2} s^{-1} Å^{-1}, while the line flux is in units of 10^{-12} erg cm^{-2} s^{-1}. The continuum varied by ±25% and the C IV line flux varied by ±15% peak to peak.

frame, and include contributions from N IV] λ1486, O III] λ1663, and Si III] λ1893, respectively. The Si IV/O IV] blend was measured between 1370 and 1440 Å. The Mg II λ2798 line flux (measured between 2725 and 2915 Å observed frame) is particularly difficult to measure given the uncertainty in continuum placement and may include a contribution from Fe II emission (§ 3.2). N V emission-line measurements are not included as this line is heavily blended with both Lyα and geocoronal Lyα emission and also exhibits a superposed N V absorption line. The errors in the emission-line fluxes and line equivalent widths were determined by disturbing the continuum fits by ±5% for the noisier spectra (i.e., the archival-low and archival-medium spectra) and by ±3% for the others. This is consistent with the root mean square variation in the continuum flux over the wavelength regions used in the determination of the continuum fits.

The C IV and Si IV absorption line equivalent widths were measured relative to a straight line drawn between the adjacent emission-line peaks. The N V absorption was measured relative to a horizontal line defined by the red emission-peak. Although physically distinct broad and narrow absorption components may exist in the archival data we have made no attempt at deblending them. Note that we do not give errors for the absorption line equivalent widths, as we consider measurement of absorption relative to some imposed line profile highly suspect based on the observed line profile variability (§ 3.2). In general however, we assume that the given values are lower limits to the true absorption.

TABLE 3

ARCHIVAL *IUE* SWP OBSERVATIONS OF NGC 3516

Archival-low	Archival-mid	Archival-high
SWP 01821	SWP 08633	SWP 24192
SWP 01840	SWP 08883	SWP 32273
SWP 06921	SWP 13425	SWP 32280
SWP 19948	SWP 14241	SWP 37274
SWP 19957	SWP 14243	SWP 37375
SWP 26811	SWP 19940	SWP 37293
SWP 26923	SWP 21257	SWP 37308
SWP 35947	SWP 24253	SWP 37327
	SWP 24344	
	SWP 24391	
	SWP 26872	
	SWP 29334	
	SWP 29340	
	SWP 30886	
	SWP 30891	
	SWP 33199	
	SWP 33203	
	SWP 33204	
	SWP 35946	

TABLE 4

ARCHIVAL *IUE* LWP OBSERVATIONS OF NGC 3516

Archival-low	Archival-mid	Archival-high
LWP 06831	LWP 02019	LWP 12042
LWP 06897	LWP 06858	LWP 12049
	LWP 09213	LWP 16524
	LWP 09215	LWP 16548
	LWP 10671	LWP 16567
	LWP 10678	

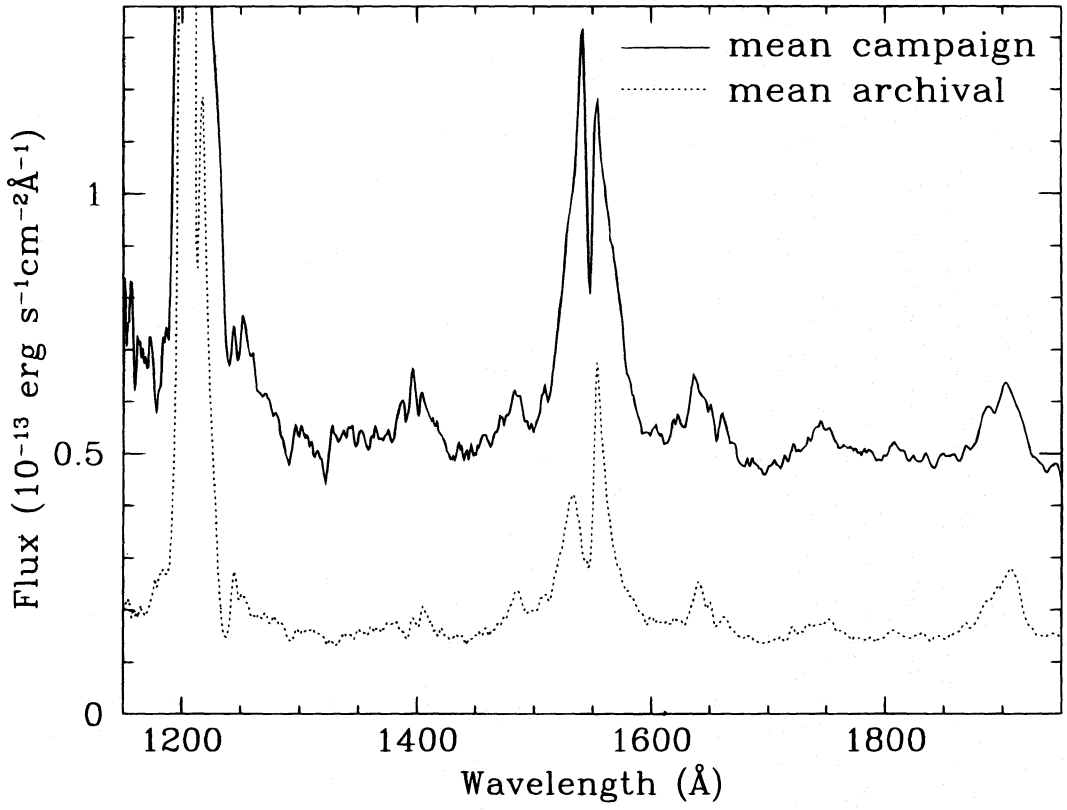

FIG. 2*a*

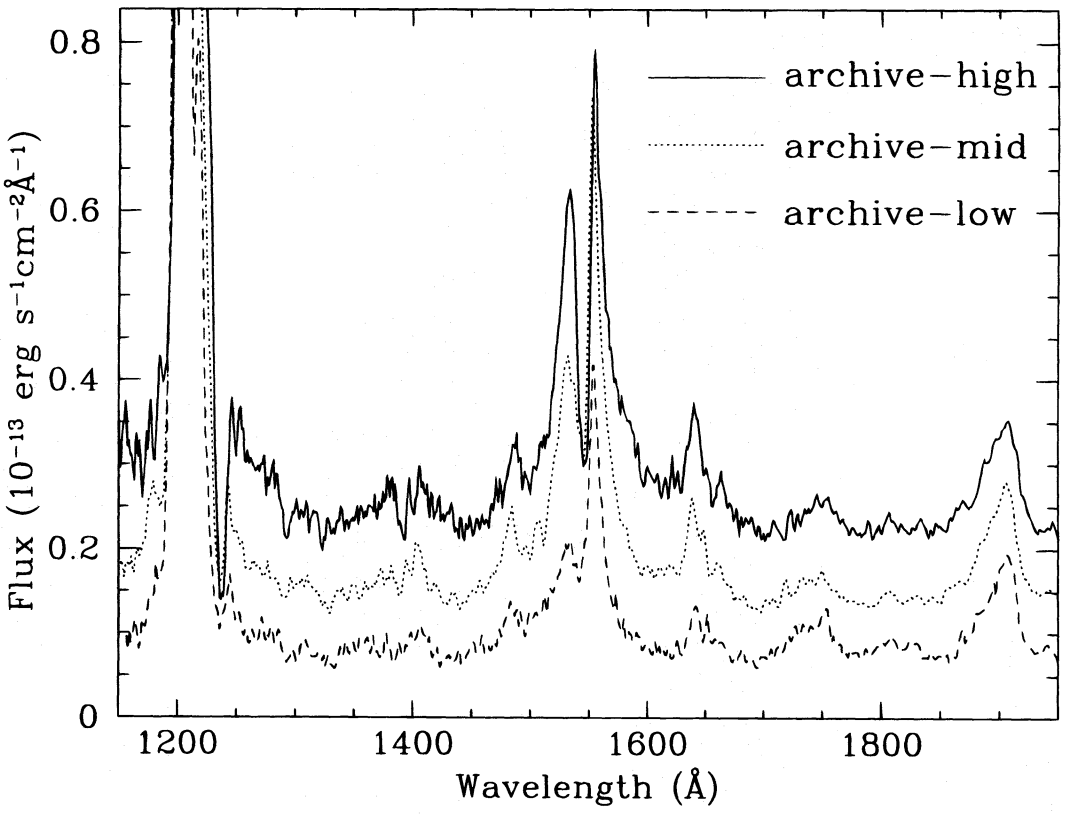

FIG. 2*b*

FIG. 2.—(*a*) Comparison of the average archival and campaign spectra for C IV. (*b*) Comparison of the archival-low, archival-medium, and archival-high state spectra for C IV. We see that during the monitoring campaign NGC 3516 was historically at its brightest state, the C IV line profile has changed dramatically, the absorption lines are weaker, and all the major emission lines are stronger.

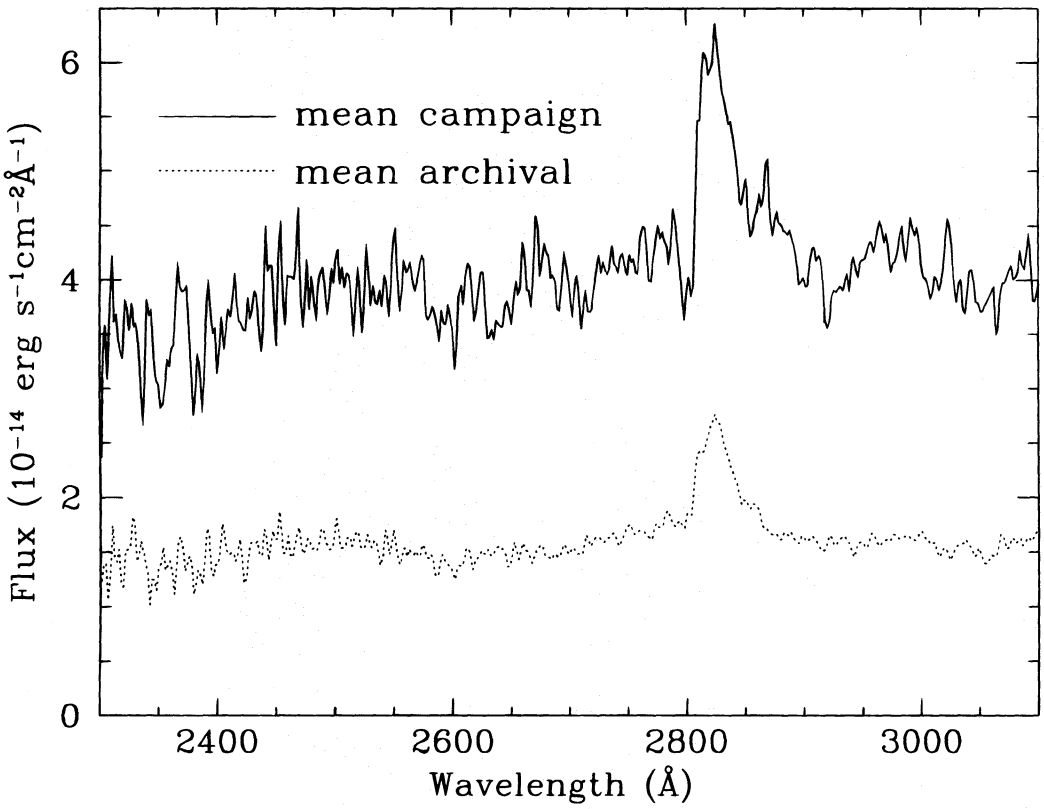

FIG. 3*a*

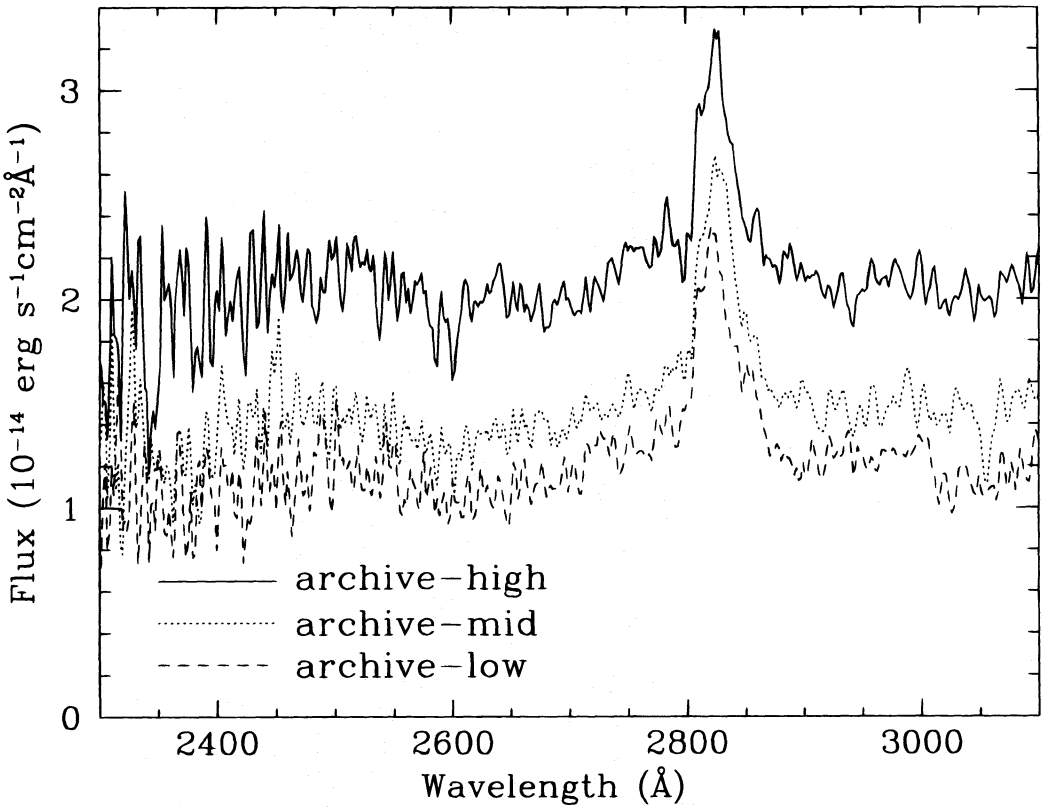

FIG. 3*b*

FIG. 3.—(*a*) Comparison of the mean archival and campaign spectra for Mg II. (*b*) A comparison of the archival-low, archival-medium, and archival-high state spectra for Mg II. As for C IV, the Mg II emission line is generally stronger when the continuum is brighter.

TABLE 5

LINE MEASUREMENTS FOR THE AVERAGE SPECTRA

Line	Line Flux[a] (10^{-13} erg cm^{-2} s^{-1})	EW[a] (Å)
Mean Archival Spectrum		
F_{cont}(1435–1450 Å)[b]	1.45 ± 0.05	...
N v absorption[c]		3.9
Si IV + O IV]	1.1 ± 0.3	$7.5^{+2.7}_{-2.0}$
Si IV λ1393 absorption		1.4
Si IV λ1402 absorption		0.6
C IV	16.6 ± 0.4	$118.6^{+6.4}_{-6.8}$
C IV absorption		6.1
He II	3.9 ± 0.4	$28.4^{+3.5}_{-3.5}$
C III]	4.2 ± 0.4	$28.4^{+3.2}_{-3.1}$
Mg II	5.8 ± 0.9	$37.7^{+7.1}_{-6.2}$
Archival-low Spectrum		
F_{cont}(1435–1450 Å)[b]	0.73 ± 0.06	...
N v absorption[c]		3.1
Si IV + O IV]	0.8 ± 0.3	$11.3^{+3.5}_{-4.3}$
Si IV λ1393 absorption		1.2
Si IV λ1402 absorption		0.6
C IV	9.9 ± 0.3	$146.3^{+7.8}_{-12.0}$
C IV absorption		5.6
He II	1.8 ± 0.3	$26.2^{+7.1}_{-4.8}$
C III]	3.9 ± 0.3	$56.0^{+7.4}_{-7.2}$
Mg II	5.9 ± 1.1	$52.0^{+12.4}_{-12.2}$
Archival-mid Spectrum		
F_{cont}(1435–1450 Å)[b]	1.39 ± 0.06	...
N v absorption[c]		3.1
Si IV + O IV]	1.5 ± 0.5	$11.1^{+4.1}_{-4.2}$
Si IV λ1393 absorption		1.6
Si IV λ1402 absorption		0.7
C IV	18.5 ± 0.6	$140.2^{+13.6}_{-12.4}$
C IV absorption		5.7
He II	4.4 ± 0.6	$33.6^{+7.1}_{-5.7}$
C III]	4.1 ± 0.6	$28.1^{+5.5}_{-4.8}$
Mg II	5.7 ± 1.4	$39.8^{+12.2}_{-10.9}$
Archival-high Spectrum		
F_{cont}(1435–1450 Å)[b]	2.25 ± 0.10	...
N v absorption[c]		5.9
Si IV + O IV]	1.6 ± 0.5	$6.9^{+0.9}_{-1.9}$
Si IV λ1393 absorption		1.8
Si IV λ1402 absorption		0.9
C IV	19.9 ± 0.6	$90.9^{+5.6}_{-6.0}$
C IV absorption		7.0
He II	5.6 ± 0.6	$25.8^{+3.3}_{-3.5}$
C III]	4.4 ± 0.5	$19.8^{+3.0}_{-2.9}$
Mg II	6.1 ± 1.1	$30.2^{+7.5}_{-6.4}$
Campaign Spectrum		
F_{cont}(1435–1450 Å)[b]	5.04 ± 0.10	...
N v absorption[c]		0.4
Si IV + O IV]	3.1 ± 1.1	$6.2^{+2.6}_{-2.3}$
Si IV λ1393 absorption		0.5
Si IV λ1402 absorption		0.4
C IV	32.3 ± 1.4	$66.6^{+5.2}_{-5.3}$
C IV absorption		2.1
He II	6.2 ± 1.3	$13.0^{+3.5}_{-2.9}$
C III]	5.7 ± 1.1	$12.0^{+2.9}_{-2.9}$
Mg II	10.2 ± 2.3	$25.3^{+8.1}_{-5.3}$

[a] Errors on the emission-line fluxes and line equivalent widths were determined by disturbing the continuum fits by ±5% for the low-state and medium-state archival spectra, and by ±3% for the others. This is consistent with the root mean square variation in the continuum flux over the regions used to determine the continuum fits.

[b] Mean continuum flux in the 1435–1450 Å bin in units of 10^{-14} erg cm^{-2} s^{-1} Å^{-1}.

[c] These values refer to the narrow absorption line EWs for the campaign data, and the sum of the narrow and broad absorption line EWs for the archival data.

It could be argued that averaging over continuum level may cause us to miss temporal changes in the line profiles. However, even with the improved extraction routine employed here, the signal-to-noise ratio is low in individual spectra. In addition the multiplicative nature of the *IUE* detector fixed pattern noise (FPN) makes previous claims for small (~5%) changes in the line profiles over small wavelength ranges suspect (e.g., Voit et al. 1987). This is particularly true near the line peaks where the absolute flux changes due to FPN will be greatest. The average archival spectra have greatly improved signal-to-noise, so although they will smear out any small intrinsic rapid variability, they should provide a reasonable view of the behavior of the spectrum as a function of continuum level. The fact that we can find an overall correlation between line profile and continuum level implies that the gross properties of the absorption and BLR emission did not change substantially during the period covered by the archival spectra.

3. RESULTS

3.1. *Time Series Analysis of the Campaign Data*

One of the aims of the campaign was to study the time-variability of the continuum source and the emission and absorption lines. From the campaign continuum and C IV light-curves shown in Figure 1 we see that NGC 3516 varied peak to peak by only ±25% in the continuum and ±15% in the C IV line.

As explained in § 2 the scattered light problem did not directly affect the SWP spectra. For SWP spectra that are badly exposed, there may be some degradation of the photometric accuracy due to the nonlinearity of the *IUE* detectors. This particularly affected the few spectra which have a low continuum level taken when the radiation background was unusually high. These spectra—SWP 47043, 47497, and 47545—were excluded from the time series analysis, together with SWP 47596 and 47607, which have very short exposure times. Because of the low amplitude of the variations compared with the data accuracy, a reliable line response function (Blandford & McKee 1982) could not be derived for C IV. Instead only a simple cross-correlation analysis was performed on the data given in Table 2.

The light-curves shown in Figure 1 suggest that the C IV emission line responds to continuum variations on relatively short timescales. Figure 4*a* (*solid line*) shows the continuum—C IV line cross-correlation function (CCF). In Figure 4*b* we show the sampling window autocorrelation function (ACF; *solid line*), which is the correlation function obtained if the continuum observations consisted entirely of white noise, the continuum ACF (*dashed line*) and the C IV line ACF (*dotted line*). Gaskell & Peterson (1987) suggested that the continuum variations are temporally well-resolved if the FWHM of the sampling window ACF is less than ~1.1 × FWHM of the continuum ACF. From our data, a comparison of the FWHM of the continuum ACF (≈6.4 days) with the FWHM sampling window ACF (≈2.6 days) suggests that the continuum variations are indeed temporally well-resolved. However, the peak correlation coefficient of the CCF (≈0.54) suggests that the line and continuum variations are only weakly correlated, with the line lagging the continuum by 4.5 days. The centroid of the CCF as measured at 30% of the peak correlation coefficient is ≈4.3 days. The archival data are too sparse to allow an extension of this analysis to earlier epochs. The derived C IV

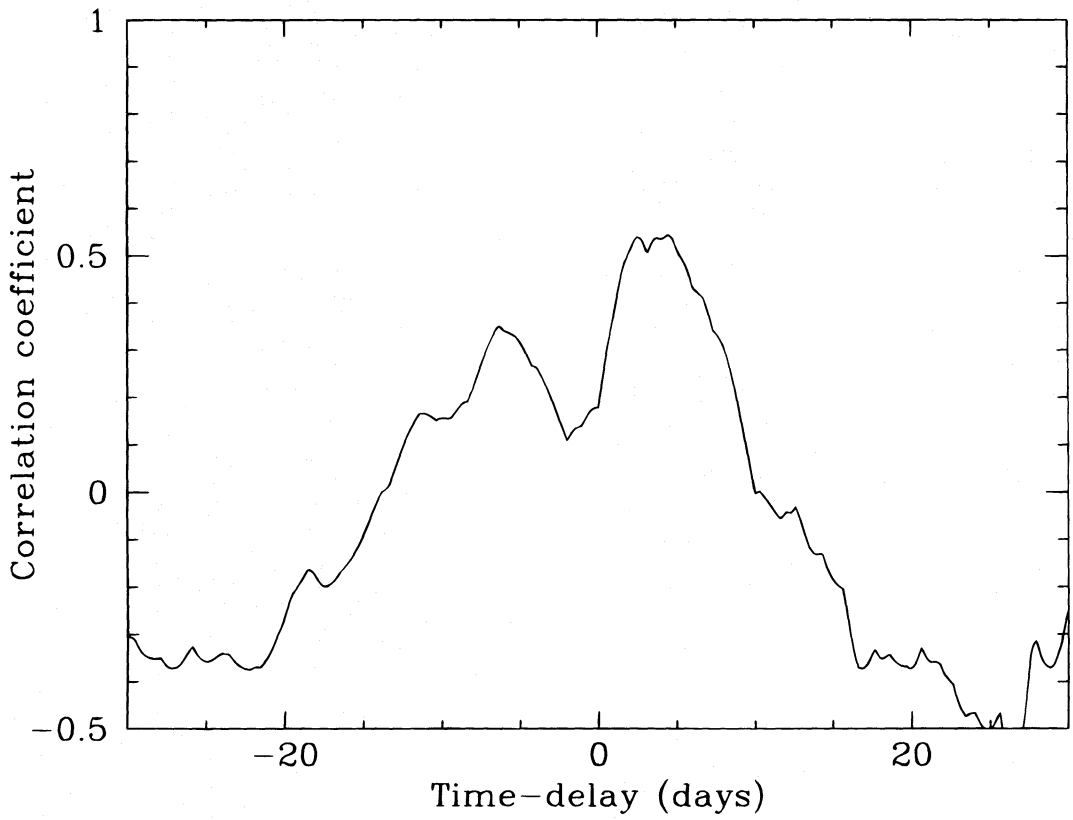

FIG. 4*a*

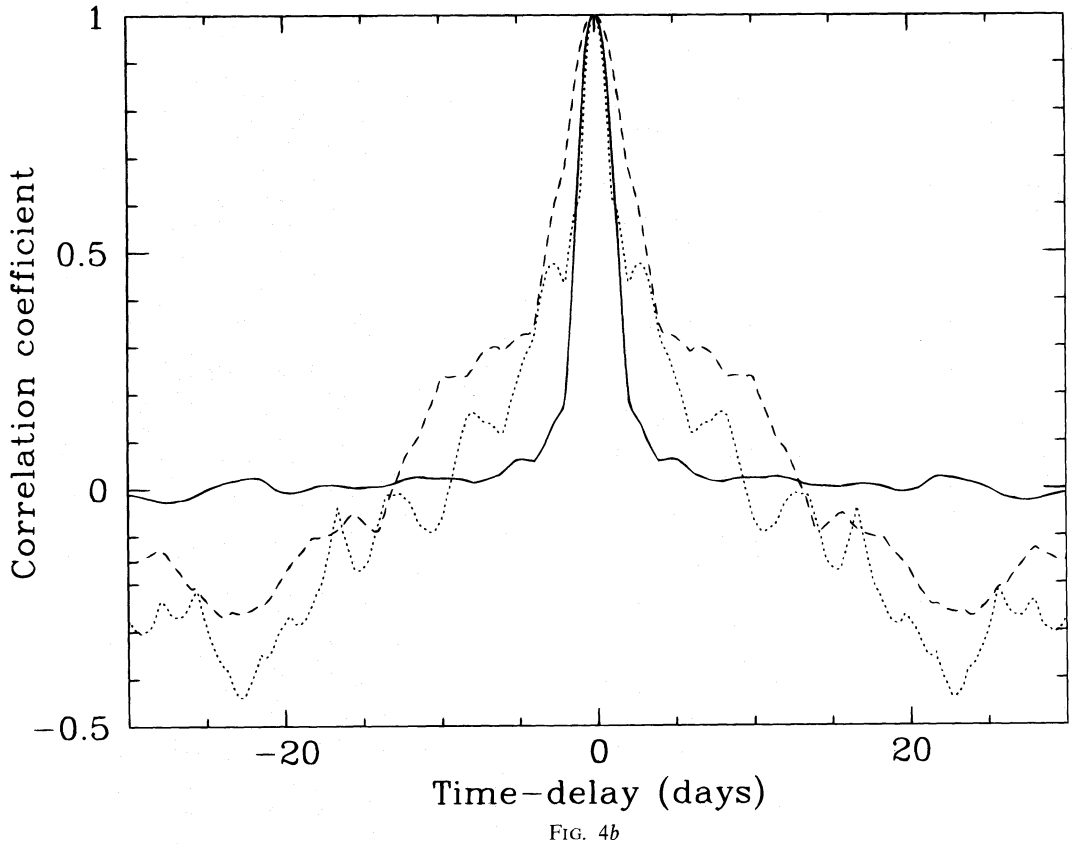

FIG. 4*b*

FIG. 4.—(*a*) Cross-correlation function (CCF) determined from all the *IUE* data on NGC 3516 (*solid line*). (*b*) Comparison of the sampling window (*solid line*) with the continuum autocorrelation function (ACF; *dashed line*) and the C IV emission line ACF (*dotted line*).

lag of 4.5 days is a factor of 2–3 smaller than that measured for the Balmer lines in NGC 3516 (11–14 days; Wanders et al. 1993; Wanders & Horne 1994). The absolute and relative values of the time-delay between the continuum, C IV, and Balmer line variations, are similar to the results found for other Seyfert 1 galaxies of comparable luminosity (Clavel et al. 1990, 1991; Reichert et al. 1994). The C IV emitting BLR is either very small or is aligned close to the line of sight.

From Figure 4*b*, the line ACF which is simply the ACF of the continuum convolved with the ACF of the response function, is found to be narrower (FWHM $\approx$ 3.5 days) than the continuum ACF (FWHM $\approx$ 6.4 days). One way to produce a narrow line ACF compared to the continuum ACF and to reduce the amplitude of the emission line response is to invoke the presence of negative responsivity gas (Sparke 1993; Goad et al. 1993), i.e., as the continuum level *increases*, the line emission *decreases*, and vice versa for a decreasing continuum (see § 3.2, eq. [1]). For C IV to have negative responsivity would require highly ionized gas, optically thin at the Lyman limit. Since NGC 3516 is in its historically brightest state, the presence of a significant amount of optically thin gas in the BLR is physically plausible. However, similar results can also be produced when the line variations are dominated by noise. If noise is not the dominant factor, simulations show that the observed response of the BLR in NGC 3516 is so extreme that the BLR would have to be dominated by negatively responding gas.

We note that the form of the CCF is sensitive to the volume emissivity distribution of the BLR clouds, and weak continuum-line correlations can be obtained by choosing an appropriate BLR geometry (B. M. Peterson, private communication). The sensitivity of the line response to the volume emissivity distribution has been discussed in detail by Robinson & Pérez (1990). However, this cannot explain the relative ACF widths.

Throughout the rest of this paper we turn our attention to the long term variability of the broad emission and absorption lines and their relationship to the nuclear continuum level.

3.2. *Comparison of the Archival and 1993 Campaign Spectra*

There are large differences between the continuum level and emission line fluxes between the mean archival and campaign spectra (Fig. 2). The mean UV continuum level at 1450 Å for the 1993 spectrum is approximately 3.5 times higher than that of the mean archival spectrum. In fact, all of the 1993 spectra have a higher continuum level than any of the individual archival spectra. In addition, and in striking contrast, *none* of the campaign spectra show the broad troughs seen in *all* of the archival spectra. A narrow, unresolved, absorption line slightly redshifted relative to the emission line peak is present in C IV and Si IV, and possibly N V (Fig. 2*a*). We will return to the implications of these variations for VAL models in § 4, but in the rest of this section we concentrate on the emission line and continuum variability.

The average spectra can be used to estimate the continuum reddening toward NGC 3516. Although the signal-to-noise ratio is low at the short-wavelength end of the LWP spectra, a 2200 Å feature is apparent. If we adopt the Galactic reddening law of Seaton (1979), the 2200 Å feature is removed and the continuum resembles a powerlaw at all continuum levels for an $E(B-V) = 0.15 \pm 0.03$. This color excess is consistent with that found by Kolman et al. (1993), exceeds that expected from our galaxy ($\approx$0.06), and implies an intrinsic column density $N_{\rm H} \sim 7 \times 10^{20}$ cm^{-2} (Bohlin et al. 1978), sufficient to produce a detectable Lyman edge. The spectra, line fluxes and equivalent widths given in this paper have not been dereddened. The UV continuum hardens with increasing continuum flux, with a dereddened powerlaw spectral index ($f_\nu \propto \nu^\alpha$) that varies from $\alpha = -2.0 \pm 0.2$ for archival-low to $\alpha = -1.0 \pm 0.2$ for the campaign.

To illustrate the relative changes in the emission lines between the archival and campaign data, Figure 5 shows the difference between the campaign and mean archival spectra (i.e., campaign–mean archival), shown in Figure 2*a*. Similar difference spectra were formed for other pairs of average spectra. All of the major emission lines are stronger in the campaign data compared to the mean archival, and generally the line fluxes increase with increasing continuum level (Table 5).

In the linear response approximation, we can quantify the line responsivity using a variable η (Goad et al. 1993). Here we define $\eta(v)$ as the fractional change in the observed line flux at observed velocity v between two spectra a and b divided by the observed fractional change in continuum level at some fiducial wavelength, i.e.,

$$\eta(v) = \frac{[L(v)_b - L(v)_a]/L(v)_a}{(C_b - C_a)/C_a} . \quad (1)$$

If the cloud density remains constant during continuum variations and the continuum shape remains fixed, the fractional change in continuum level gives the fractional change in ionization parameter U. Clearly $\eta(v)$ is an average over all parts of the BLR contributing line emission at that observed velocity. In theory some information on the variation of η with position within the BLR can be extracted by adopting a model relating velocity to position. In Figures 6*b*–6*e*, $\eta(v)$ is shown for the C IV line for cases in which a and b represent the archival-low and archival-mid, archival-mid and archival-high, archival-high and campiagn, and mean archival and campaign spectra, respectively. The normalized C IV profile for the archival-mid spectrum is shown in Figure 6*a* for comparison. We also calculated mean line responsivities averaged across the entire BLR using the total line fluxes given in Table 5.

Comparing the difference spectra, mean total line responsivities, and the $\eta(v)$-values, it is clear that the variability characteristics of the broad emission lines in NGC 3516 vary with continuum level. From the low to medium continuum level the responsivity is fairly uniform across the C IV line with $\eta \sim 1$ (Fig. 6*b*). There is an excess response—a "red feature"—in the far red wing of C IV ($>$5000 km s^{-1}), where $\eta \sim 2$, which suggests the existence of an underlying asymmetry either in the gas distribution, the radiation pattern of the ionizing continuum source, or possibly both. Although the C IV line equivalent width begins to drop at high continuum levels, the increased flux suggests that the dip in $\eta(v)$ in the blue C IV line core (Fig. 6*c*) is most likely due to a change in strength of the broad trough, and not due to the presence of negative responsivity gas. As the continuum increases above the medium level the C IV responsivity drops in the line wings and $\eta \sim 0.3$ at high continuum levels (Fig. 6*d*). Thus, the wings appear to saturate when the continuum is very bright. The red feature

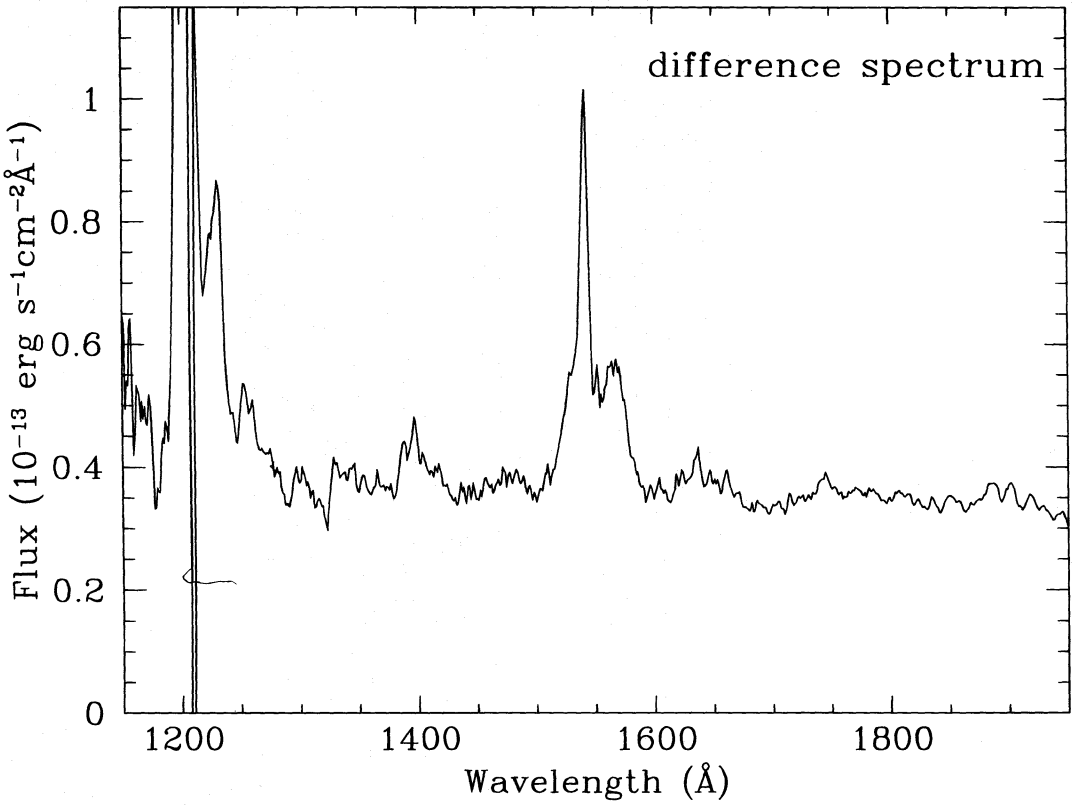

FIG. 5.—Difference between the campaign and mean archival spectra (campaign—mean archival) for C IV. The difference spectrum shows a clear deficit of response redward of line center.

appears to saturate more slowly than the blue C IV wing, but does saturate above the high continuum level. The lower $\eta(v)$ in the red C IV line core may be due to dilution by narrow line emission/absorption or a lack of variable emission (§ 4.3). Figure 6*e*, which shows the $\eta(v)$ formed between the mean campaign and mean archival spectra, indicates that on average, the main difference in response between the campaign and archival data is an increased response over a narrow range in velocity space ($\sim$3000 km s^{-1}) centered $\sim$1500 km s^{-1} blueward of line center.

The N V blue wing is badly blended with Lyα, but the red wing appears to vary in a similar way to He II. At low continuum levels N V is weak, with $\eta \sim 1$, declining to $\sim$0.6 at high continuum levels. In contrast to C IV, $\eta \sim 0.13$ for C III] at all continuum levels. The Si IV, O IV] blend is weak and badly affected by absorption at low to medium continuum levels, but we estimate $\eta < 1$ at high continuum levels. Given the uncertainty in continuum placement, the Mg II responsivity is low for the archival LWP data. The Mg II line appears much stronger in the two campaign LWP spectra (Fig. 3*a*), implying $\eta \sim 0.6$ at high continuum levels. However, the extra emission appears mainly in the red wing of Mg II and may be due to an increase in Fe II emission. Several other weak emission features are seen in the campaign data at wavelengths corresponding to expected Fe II lines (Grandi 1981).

Galactic Mg II absorption can clearly be seen in the blue wing of Mg II in the LWP campaign and archival-high spectra. Similarly, galactic absorption lines with EWs of $\sim$0.5 Å can be seen in the mean campaign spectrum at 1302 and 1334 Å. Kolman et al. (1993) suggest that the slightly asymmetric shape of the Mg II line at some epochs may be due to a weak low-ionization VAL. However, given the shape of the C IV line in the campaign data and the suggested Fe II emission, we find no convincing evidence for a Mg II VAL at any continuum level. Higher spectral resolution data are required to confirm this conclusion. There is also no evidence for a narrow intrinsic Mg II absorption line at the same redshift as in C IV.

Based on the BLR models discussed by Goad et al. (1993, 1994), the observed combination of low responsivity and the declining reprocessing efficiency at higher continuum levels are consistent with models in which the emission line gas has both a low optical depth at the Lyman limit and a high ionization parameter. This conclusion is consistent with the suggestion of optically thin gas to explain the comparative widths of the C IV and continuum ACFs (§ 3.1) and the low C III]/C IV emission line ratio.

4. VARIABLE BROAD ABSORPTION OR A PREFERRED BLR GEOMETRY?

The profile variations observed in NGC 3516 have been discussed previously mainly in terms of a VAL (§ 4.1). Although we consider this model to be the most likely, we also note another possibility, namely that the broad absorption troughs may have been "filled in" during the campaign by an additional emission component (§ 4.2). This additional emission component cannot alone explain the profile variability seen in *IUE* archival data, and does not remove the need for a VAL, but may indicate a preferred BLR geometry and velocity field for the line-emitting gas in this object. The merits of each of these models are discussed below.

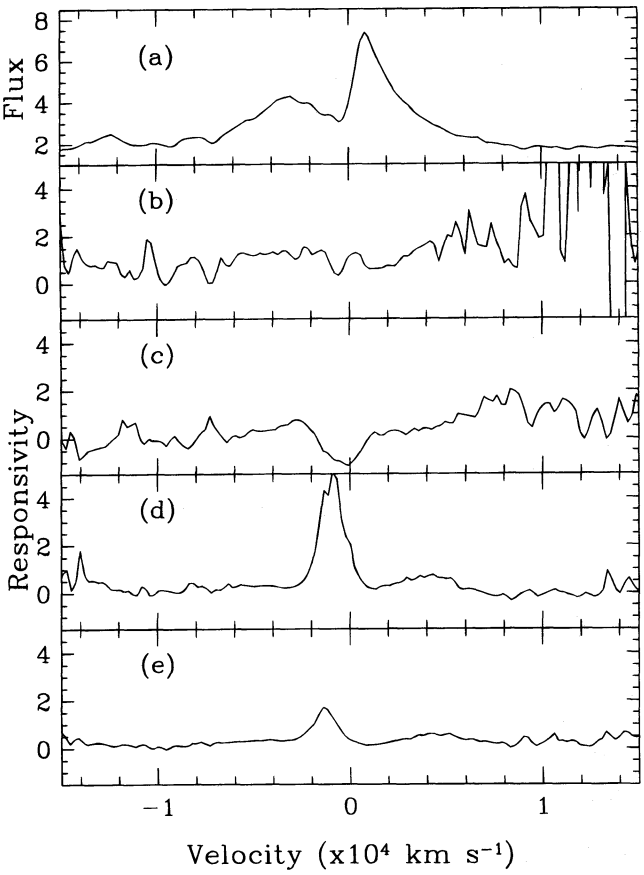

FIG. 6.—Line responsivity $\eta(v)$ plots for C IV, where $\eta(v)$ is as defined in eq. (1). The two spectra, a, b, in each case correspond to: (*b*) the archival-low and archival-mid; (*c*) the archival-mid and archival-high; (*d*) the archival-high and campaign; and (*e*) the mean archival and campaign. Panel (*a*) shows the archival-mid spectrum to identify those regions of velocity space in which the variations occur.

4.1. *The VAL Model*

Previous work based on the archival *IUE* spectra has led to the supposition that the deep troughs in the C IV λ1549, N V λ1240, and Si IV λ1400 lines are due to ionized, absorbing gas covering a wide velocity range which cover a large fraction of the broad emission line region in NGC 3516 (Voit et al. 1987; Walter et al. 1990). Walter et al. found an anticorrelation between the column density of C IV absorbers and continuum luminosity which persists for a couple of years, before breaking down and reappearing later but with a different normalization. They attributed the variable normalization of the anticorrelation to different clouds crossing the line of sight, whereas the anticorrelation was due to the C^{3+} ionization front moving in response to variations in the continuum luminosity within a variable density absorbing cloud, with the variations in the ionization front position being on the same scale as the cloud size. Assuming the short variability timescales are attributed to recombination, they deduced a characteristic cloud density $\sim 10^{4-5}$ cm^{-3} and size $\sim 10^{15}$ cm. Walter et al. further found that the absorption troughs consist of two components—a nonvariable narrow absorption line near zero rest-frame velocity that is unresolved in the *IUE* spectra, and a blueshifted, broad, VAL. Kolman et al. (1993) also attributed variations in the observed VAL strength to changes in the ionizing flux. They estimated the distance of the VAL gas from the continuum source as less than 9 pc, with a most probable location as being optically thin clouds within the BLR. They also find that the properties of the VALs in NGC 3516 are consistent with it being a low luminosity version of a BAL quasar.

Although strong C IV λ1549, N V λ1240, and Si IV λ1400 troughs were seen in all of the individual archival spectra we examined, we found no clear evidence to support previous claims of small amplitude rapid variations (see Walter et al. 1990), and hence cannot reliably constrain the gas density. In fact, for low U models, the expected variation in absorption line equivalent width due to the observed continuum variations is relatively small. Thus detection of such small variations would be difficult, given that the uncertainty in measuring the absorption line equivalent width (assuming some underlying emission-line profile; § 2.4) is very likely to be large. As noted in § 2.4, analysis of the individual *IUE* spectra is plagued with difficulty due to random and fixed-pattern noise. In addition, intrinsic emission-line profile variability may cause apparent changes in the profile on small timescales due to the fast response of the emission lines (§ 3.2). Therefore, although we cannot rule out such changes, we will concentrate on the average spectra. Thus, rather than investigating the physical characteristics of the emission/absorbing gas from its short-term variability (~days), we use the average spectra to determine more general properties of the line emitting/absorbing gas (e.g., changes in the gas distribution, and reprocessing efficiency over timescales of ~years).

The average archival spectra provide little evidence for a variation in the total range in velocity covered by the absorption (see Voit et al. 1987). The absorption troughs have a very similar width in all the average archival spectra (see Fig. 2*b*), extending from -3000 ± 300 to $+800 \pm 200$ km s^{-1}. However, the C IV trough does have a broader flatter bottom in the archival-mid and archival-high spectra, implying an increase in optical depth at lower velocities when the continuum is higher. The measured N V, C IV, and Si IV equivalent widths (Table 5) all show a moderate increase with continuum level. This trend may be an artifact produced by systematically underestimating the line flux at low continuum levels. However, despite these problems, any intrinsic variation in the absorption line strengths in the archival spectra are less than half the rate of change of the continuum level, and hence U if the continuum shape is fairly constant.

Standard photoionization models for BAL QSO suggest that the absorbing gas is of moderate ionization with ionization parameter $U \sim 0.01$–0.1. For such models (e.g., Smith & Penston 1988; Barlow 1993) the expected variation in absorption equivalent widths due to the range in continuum level (factor of 4) in the archival spectra is of order a factor of 2 or less, consistent with the observed variations. The sense of the global change inferred from the average archival spectra (equivalent widths increasing with increasing continuum level) implies that $U \sim 0.01$. Given the factor of 2 increase in the continuum level between the archival-high and campaign data, the standard BAL QSO type models for the absorber imply that sufficient atoms should have remained in the relevant ionization state to produce detectable VALs in the campaign data, which are clearly not observed.

In an attempt to link UV and "warm" X-ray absorbers, it has been suggested that the UV absorption lines observed in some quasars and Seyfert 1 galaxies are due to ionic

species which are merely trace fractions in gas far more highly ionized ($U \sim 1$) than is usually assumed for the BAL QSOs (Mathur et al. 1994, 1995). In these models the decrease in fractional abundance for species such as C^{+3} and N^{+4} could be large for small changes in U. Soft X-ray observations suggest NGC 3516 contains a warm absorber (Kolman et al. 1993) consistent with the UV absorption, but the small observed variations in the VAL equivalent widths and strong low ionization Si^{+3} absorption seen in the archival data argue against such a highly ionized model. We therefore conclude that, in the context of a VAL model, the most likely cause for the reduction in VAL strength in the campaign data is due to dissipation or bulk motion of the absorbing gas away from the line of sight. This supports the conclusions drawn by Walter et al. (1990), concerning bulk motions of the absorbing gas, and indicates that the VAL region in NGC 3516 is highly dynamic.

Since we have no information concerning the short-term variability of the absorbing gas (due to averaging of the archival and campaign spectra), we cannot easily constrain the density of the absorber and thus its size. If the density estimates of Walter et al. are correct ($N_e \sim 10^5$ cm^{-3}), then together with the absence of a Mg II VAL, which places an upper limit on the hydrogen column density of $N_H < 10^{20.5}$ cm^{-2}, an upper limit on the absorbing cloud size of less than 10^{15} cm can be derived. For transverse cloud velocities of $\sim$1500 km s^{-1} the crossing time for the absorber is $\sim$2–3 months. Clouds moving obliquely across our line of sight may persist for much longer periods ($\sim$years). The elapsed time between the last of the archival observations and the beginning of the campaign, is in this instance large enough for the absorber to have moved out of our line of sight.

The available data for NGC 3516 do not allow us to determine the exact nature of the VAL. For example, whether it comprises a set of clouds along the line of sight or a wind. Neither do the data accurately locate the VAL relative to the BLR. The fact that the troughs are clearly deeper than the continuum level (e.g., N V in the archival-high spectrum; see Fig. 2*b*) implies that at least some of the absorbing gas covers the BLR. This could be due merely to the narrow absorption component present in the campaign data and previously inferred by Walter et al. (1990), but Walter et al. find their spectral fits require the VAL to at least partially cover the BLR. If we assume the VAL gas originates outside the BLR, then a possible location is the fragmenting surface of a surrounding molecular torus (Heckman et al. 1989; Weymann et al. 1991; Kolman et al. 1993). Although we are not viewing the central continuum source and BLR of NGC 3516 through the entire torus, if our line of sight skims its surface, we may see absorption due to a wind and/or cloud fragments ablated off of the torus. As this situation is intrinsically highly dynamic, variations in the amount of absorber along the line of sight are not unexpected. The complex extended narrow-line region and radio structure of NGC 3516 imply we are viewing this object at a large angle from the radio axis (Goad & Gallagher 1987; Miyaji, Wilson, & Perez-Fournon 1992). Interestingly, the extended structure shows several "blobs" of emission, and Miyaji et al. suggest NGC 3516 may undergo sporadic ejection of material. Although this material is being ejected along a different direction to the UV absorber, it may be related and further indicates the dynamic nature of NGC 3516.

4.2. *A Preferred BLR Geometry—Evidence for a Biconical Outflow?*

A comparison of the campaign and archival spectra with previously published BLR models (see Pérez, Robinson, & de la Fuente 1992; O'Brien, Goad, & Gondhalekar 1994; Robinson 1995) suggests that at least in a qualitative sense the observed C IV emission line profile variation seen in NGC 3516 in 1993 is consistent with emission from a biconical BLR or a beamed continuum source. Such a model has been proposed recently to explain the C IV emission line variability in NGC 5548 (Wanders et al. 1995).

A biconical model cannot however explain the archival data on its own. For example, the extension of the N V line trough below the continuum level in the archival-high spectrum cannot be produced in a bicone without invoking an additional contribution from an absorption component. Thus, if a bicone is present, it must usually be weak, only appearing in 1993 due to a change in behavior perhaps associated with the unusually high continuum level. If we adopt this interpretation, then in terms of the reverberation model, the difference in response of the red and blue sides of the broad emission-lines between the archival and campaign spectra implies that the BLR is very extended in size and lies close to the line of sight.

One plausible model for the BLR is emission from clouds moving in a biconical outflow, which may or may not be relativistic (Orr & Browne 1982), and whose axis is aligned close to the line of sight. Alternatively, the BLR may be comprised of a spherically symmetric outflow, irradiated by an anisotropic continuum source, and whose strongest component lies close to the line of sight. Such a situation might arise if the continuum emission originates from the surface of an accretion disk with a low line of sight inclination (Netzer 1987; Wanders et al. 1995). In the bicone model a minimum distance of the gas producing the red C IV peak can be estimated by assuming the continuum increased to the campaign level early in 1993 February. If profile variations are caused by reverberation effects, then the lack of response for the red peak during the three-month campaign then implies a distance of the red emitting gas from the continuum source of at least 1.5 light-months.

If we assume that C IV remains responsive when the continuum increases, the weaker response in the line core is then consistent with a geometrically thick BLR in which the velocity *decreases* with increasing distance from the central ionizing continuum source. Conversely, it the clouds are unresponsive (i.e., saturated) in the C IV line (§ 3.2), a suggestion supported by the decline in EW with increasing continuum level, then the profile variations are consistent with a geometrically thick BLR in which the velocity *increases* with increasing distance from the central ionizing continuum source. For example, Figure 7 shows that at least in a qualitative sense, the low-state (*lower panel*) and high-state (*upper panel*) spectra can be modeled by emission from clouds moving radially outward in a biconical flow. For the model shown here, the clouds are confined to a biconical region with semi-opening angle $\omega = 30°$ and line of sight inclination $i = 60°$. The BLR is assumed to be spatially extended with a ratio of inner to outer radius, $R_{in}/R_{out} = 0.1$, while the velocity law is modeled as a Hubble-type flow [i.e., $v(r) \propto r$]. For the radial emissivity distribution [$\epsilon(r)$] we assume a simple power-law with radius such that $\epsilon(r) \propto r^{-3}$. In the high state the material is assumed to be

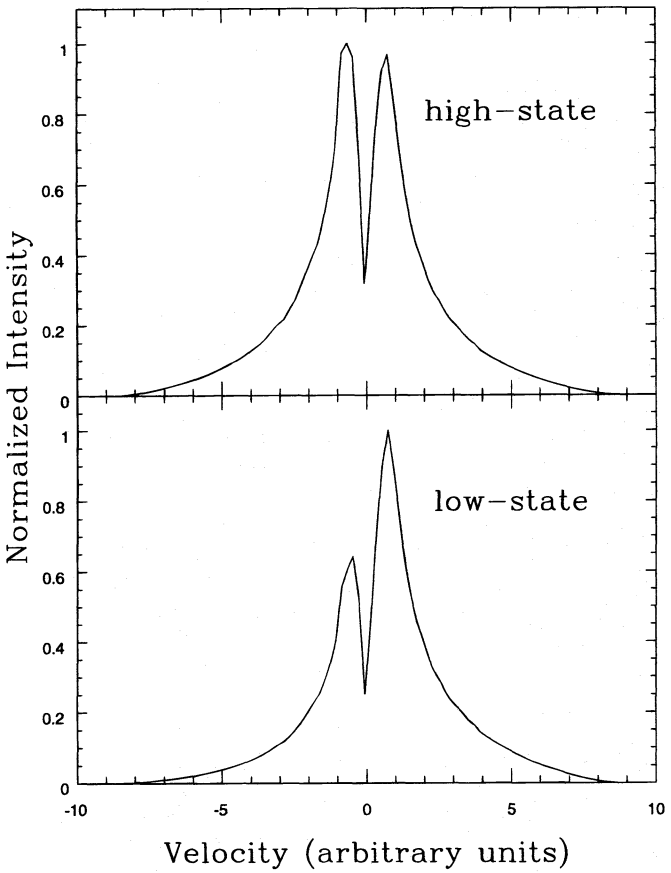

FIG. 7.—Example model line profiles for the high state (*upper panel*) and low state (*lower panel*) C IV. The model comprises a biconical Hubble-type outflow ($v \propto r$), spanning a factor of 10 in radius, with a cone semi-opening angle $\omega = 30°$, inclined at an angle $i = 60°$ with respect to the observers line of sight. The differential luminosity is given by $dL(r) \propto r^{-1}\,dr$, and is normalized such that the source is totally covered when looking directly into the cone.

unresponsive in the C IV line and radiates isotropically, while in the low state the material is optically thick in the C IV line and radiates anisotropically, with an anisotropy factor $F = 0.8$ (O'Brien et al. 1994), where F is the ratio of the inward to total emission line flux. A simple test of this model is that variations in the line profile will propagate from the blue wing to the red wing of the line on the order of the light-crossing time of the BLR. Unfortunately, the relatively poor temporal sampling and low signal-to-noise ratio of the *IUE* spectra means that we are unable to distinguish between ordered or chaotic velocity fields in this object.

If on the other hand, reverberation effects are not responsible for the observed line profile variations between the mean archival and campaign spectra, then in the context of these models, line profile variations are due to either changes in the cloud covering fraction, changes in the continuum beam opening angle and/or changes in the continuum beam orientation with respect to the observers line of sight.

Clearly more data with higher spectral resolution and higher signal-to-noise ratio are required to constrain both the VAL and bicone hypotheses. Currently scheduled *HST* observations should provide such data. If the disappearing VAL explanation is correct, then there is no particular reason to expect the VAL to return to its previous strength when the continuum flux declines from its record high level seen during 1993. There are indications that this is the case from new *IUE* data taken in 1994/1995, which is currently being reprocessed. In contrast, if the bicone is a stable structure, then the trough should return when the continuum declines. To check the distance of the BLR gas implied by the bicone model we require an estimate of the ionization parameter in the blue emission peak, which in turn requires much better constraints on the other emission line profiles. The narrow blue peak is not seen in N V, He II, or C III], although it's absence in C III] could just indicate a low optical thickness. The *HST* data should provide accurate line profiles, as well as providing the width of the narrow absorption line.

5. CONCLUSIONS

The Seyfert 1 galaxy NGC 3516 was monitored using *IUE* during 1993 to investigate the emission and absorption line variability. We have presented the first results of the campaign, which are summarized as follows:

1. The UV continuum level throughout the 1993 campiagn was higher than in all the archival *IUE* spectra. The mean 1993 continuum level was about a factor of 3 higher than in the mean archival spectrum.

2. Correlated low-amplitude UV continuum and C IV λ1549 broad emission line variability occurred during 1993. The UV continuum varied peak to peak by $\pm 25\%$, while C IV varied by $\pm 15\%$. A cross-correlation analysis shows that the C IV variations lag those of the UV continuum by ~ 4.5 days, consistent with results found for other Seyfert 1 galaxies of comparable luminosity. An analysis of the archival data shows that the strength of all of the major broad emission lines in NGC 3516 increase with increasing UV continuum level, although emission, particularly in the wings, saturates at very high levels.

3. A dramatic change occurred in both the strength and shape of the emission line profiles in 1993 compared to the *IUE* archival spectra. The 1993 spectra show no trace of broad troughs due to absorbing gas, although narrow absorption lines slightly redshifted relative to the emission line peaks are present in N V λ1240, Si IV λ1400, and C IV. The strong blue emission peak seen clearly in C IV has not been seen in NGC 3516 before, nor in any other AGNs with intrinsic VALs.

Although points (1) and (2) are in agreement with the reverberation model of the BLR, the observed line profile variability is inconsistent with a simple linear response emission and absorption line model. Rather a change has occurred in the behavior of NGC 3516. We have discussed two possible explanations for this change: a reduction in the amount of absorption or an increase in emission confined to a narrow projected velocity range.

Although the archival spectra are consistent with the standard, low-ionization, BAL QSO model for the UV absorption lines, the reduction in the strength of the line troughs in 1993 is not in agreement with the model predictions. The data imply therefore that the absorbing gas previously present has somehow been dissipated, indicating a dynamic source for the gas, possibly the surface of a molecular torus. This may be related to the sporadic ejection of material from the nucleus previously proposed based on optical and radio images.

If an extra emission component has appeared, effectively filling in the absorption trough, it affects only a narrow projected velocity range during a period when the UV con-

tinuum is unusually strong. We have discussed one possibility, namely a biconical model in which the biconical emission component has greatly increased its relative contriubtion to the line profile in 1993.

Further higher-quality data are required to clearly distinguish between these possibilities. We are currently acquiring such data with the *Hubble Space Telescope*, and these data together with more detailed models will be presented in a future publication.

We are especially grateful to all the staff at *IUE* Goddard and *IUE* Vilspa who overcame many difficulties in acquiring the data. A. K. and M. R. G. acknowledge the support of NAG 5-2111 for financial support. Some of the data analysis was performed on Starlink computer facilities funded by PPARC at UCL and Oxford. A. R. thanks the Royal Society for financial support. I. W. would like to thank STScI for its hospitality during the early stages of this work. M. R. G. would also like to thank the Department of Physics, Oxford, for its hospitality during the completion of this work. Finally, we would also like to thank the anonymous referee for comments which have greatly enhanced the clarity of the work presented here.

REFERENCES

Barlow, T. A. 1993, Ph.D. thesis, UCSD
Blandford, R. D., & McKee, C. F. 1982, ApJ, 225, 419
Bochkarev, N. G., Shapovalova, A. I., & Zherov, S. A. 1990, AJ, 100, 1799
Bohlin, R. C., & Grillmair, C. J. 1988, ApJS, 68, 487
Bohlin, R. C., Harris, A. W., Holm, A. V., & Gry, C. 1990, ApJS, 73, 413
Bohlin, R. C., Holm, A. V., Savage, B. D., & Drake, J. F. 1978, ApJ, 224, 132
Bohlin, R. C., Holm, A. V., Savage, B. D., Snijders, M. A. J., & Sparks, W. M. 1980, A&A, 85, 1
Bromage, G., et al. 1985, MNRAS, 215, 1
Carini, M., & Weinstein, D. 1992, NASA *IUE* Newsletter, 49, 5
Cassatella, A., Barbero, J., & Benvenuti, P. 1985, A&A, 144, 335
Cherepashchuck, A. M., & Lyutyi, V. M. 1973, Astrophys. Lett., 13, 165
Clavel, J. 1991, in Variability of Active Nuclei, ed. H. R. Miller & P. J. Wiita, (Cambridge: Cambridge Univ. Press), 301
Clavel, J., et al. 1990, MNRAS, 246, 668
———. 1991, ApJ, 366, 64
Fabian, A., et al. 1994, in New Horizons in X-Ray Astronomy, ed. F. Makino & T. Ohashi (Tokyo: Universal Academy Press), 573
Gaskell, C. M., & Peterson, B. M. 1987, ApJS, 65, 1
Goad, J. W., & Gallagher, J. S. 1987, AJ, 94, 640
Goad, M. R., O'Brien, P. T., & Gondhalekar, P. M. 1993, MNRAS, 263, 149
———. 1994, ASP Conf. Ser. 69, Reverberation Mapping of the Broad-Line Region in Active Galactic Nuclei, ed. P. M. Gondhalekar & B. M. Peterson (San Francisco: ASP), 315
Grandi, S. A. 1981, ApJ, 251, 451
Hammann, F., Korista, K. T., & Morris, S. L. 1993, ApJ, 415, 541
Heckman, T. M., Blitz, L., Wilson, A. S., Armus, L., & Miley, G. K. 1989, ApJ, 342, 735
Kinney, A. L., Bohlin, R. C., & Neill, J. D. 1991, PASP, 103, 694
Kolman, M., et al. 1993, ApJ, 403, 592
Koratkar, A., & Gaskell, C. M. 1991a, ApJS, 75, 719
———. 1991b, ApJ, 370, L61
Korista, K. T., et al. 1992, ApJ, 401, 529
Korista, K. T., et al. 1995, ApJS, 97, 285
Kriss, G. A., et al. 1992, ApJ, 392, 485
Krupper, J. S., Urry, C. M., & Canizares, C. R. 1990, ApJS, 74, 347
Mathur, S., Elvis, M., & Wilkes, B. 1995, ApJ, 452, 230
Mathur, S., Wilkes, B., Elvis, M., & Fiore, F. 1994, BAAS, 184, 1706
Miyaji, T., Wilson, A. S., & Perez-Fournon, I. 1992, ApJ, 385, 137
Netzer, H. 1987, MNRAS, 225, 57
Nichols-Bohlin, J. 1993, NASA *IUE* Newsletter, 51, 31
O'Brien, P. T., Goad, M. R., & Gonhalekar, P. M. 1994, MNRAS, 268, 845
O'Brien, P. T., & Harries, T. 1991, MNRAS, 250, 133
Orr, M. J. L., & Browne, I. W. A. 1982, MNRAS, 200, 1067
Pérez, E., Robinson, A., & de la Fuente, L. 1992, MNRAS, 256, 103
Peterson, B. M. 1993, PASP, 105, 247
Reichert, G. A., et al. 1994, ApJ, 425, 582
Robinson, A. 1995, MNRAS, 272, 647
Robinson, A., & Perez, E. 1990, MNRAS, 244, 138
Seaton, M. J. 1979, MNRAS, 187, 73P
Shull, J. M., & Sachs, E. R. 1993, ApJ, 416, 536
Smith, L. J., & Penston, M. V. 1988, MNRAS, 235, 551
Sparke, L. S. 1993, ApJ, 404, 570
Stocke, J. T., et al. 1992, ApJ, 396, 487
Teays, T. J., & Garhart, M. P. 1990, NASA *IUE* Newsletter, 41, 94
Ulrich, M.-H. 1988, MNRAS, 230, 121
Ulrich, M.-H., & Boisson, C. 1983, ApJ, 267, 515
Voit, G. M., Shull, J. M., & Begelman, M. C. 1987, ApJ, 316, 573
Walter, R., Ulrich, M.-H., Courvoisier, T. J.-L., & Buson, L. M. 1990, A&A, 233, 53
Wanders, I., et al. 1993, A&A, 269, 39
———. 1995, ApJ, submitted
Wanders, I., & Horne, K. 1994, A&A, 289, 76
Weymann, R. J., Morris, S. L., Foltz, C. B., & Hewett, P. C. 1991, ApJ, 373, 23
Zheng, W., Binette, L., & Sulentic, J. W. 1990, ApJ, 365, 115